Quantifying the Reactive Uptake of OH by Organic Aerosols in a Continuous Flow Stirred Tank Reactor

Dung L. Che,[1,2] Jared D. Smith,[1] Stephen R. Leone,[1,2] Musahid Ahmed[1] and Kevin R. Wilson[1,*]

[1]*Chemical Sciences Division, Lawrence Berkeley National Laboratory, Berkeley, CA 94720*
[2]*Departments of Chemistry and Physics, University of California, Berkeley, CA 94720*

ABSTRACT

Here we report a new method for measuring the heterogeneous chemistry of sub-micron organic aerosol particles using a continuous flow stirred tank reactor. This approach is designed to quantify the real time heterogeneous kinetics, using a relative rate method, under conditions of low oxidant concentration and long reaction times that more closely mimic the real atmosphere. A general analytical expression, which couples the aerosol chemistry with the flow dynamics in the chamber is developed and applied to the heterogeneous oxidation of squalane particles by hydroxyl radicals (OH) in the presence of O_2. The particle phase reaction is monitored via photoionization aerosol mass spectrometry and yields a reactive uptake coefficient of 0.51 ± 0.10, using OH concentrations of 1 – 7 x 10^8 molec·cm^{-3} and reaction times of 1.5 – 3 hours. This uptake coefficient is larger than that found for the reaction carried out under high OH concentrations (~ 1 x 10^{10} molec·cm^{-3}) and short reaction times in a flow tube reactor. This difference suggests that oxidant concentration and reaction time are not interchangeable quantities in reactions of organic aerosols with radicals. In general, this approach provides a new way to examine how the chemical aging of organic particles measured at short reaction times and high oxidant concentrations in flow tubes might differ from the long reaction times and low oxidant levels found in the real atmosphere.

*correspondence to: K. R. Wilson (krwilson@lbl.gov)

I. INTRODUCTION

Organic material is a major component of atmospheric aerosols, accounting for 20 – 90% of the aerosol mass in the lower troposphere.[1, 2] The oxidation of organic aerosols, a process also known as aging, can modify the physical and chemical properties of aerosols, which can in turn influence climate, the hydrologic cycle, visibility and human health.[3-7] Many fundamental aspects of heterogeneous aging are still not well understood. Thus, quantifying the oxidation rate of organic aerosol particles over a range of oxidant concentrations and reaction timescales is imperative to obtain a better understanding of the transformation mechanisms of atmospheric particles and to better assess the overall chemical role that organic aerosols play in the atmosphere.

Laboratory studies of organic aerosol aging primarily focus on the oxidation of simple organic particles or model systems to better understand the fundamental mechanisms that control the heterogeneous chemistry of more complex ambient aerosols. Many of these studies use flow tubes,[8-15] where high oxidant levels are required to measure heterogeneous kinetics in short reaction times. The short timescales (typically ranging from a few seconds to minutes) and high oxidant concentrations in flowtube experiments could be problematic for diffusion-limited reactions since particles may not be well mixed during such short reaction times.[16] Furthermore, secondary chemical reactions can take place within the particle itself and become competitive with the heterogeneous reaction rate only at low oxidant concentrations.[39] This could lead to situations in which the reaction time and the oxidant concentration are not linearly related quantities. Thus, it remains unclear how well these flow tube laboratory conditions mimic the real atmosphere where particles are exposed to much lower oxidant concentrations for long timescales - days to weeks. It is therefore important to develop new experimental methods to

examine chemical aging mechanisms over longer timescales using lower oxidant concentrations to better understand how experimental results obtained from flow tube measurements relate to the real atmosphere.

In the atmosphere hydroxyl radicals (OH) ([OH] ~ 1 x 10^6 molec·cm^{-3}) are expected to play a central role in the aging processes of organic aerosols.[17] Heterogeneous reactions are quantified by the reactive uptake coefficient, γ, which is generally defined as the fraction of OH collisions with a particle that yield a reaction. The heterogeneous oxidation of organic compounds by OH in the presence of O_2 has been found to be highly efficient. For example, Esteve et al. used a relative rate kinetic method to examine the heterogeneous reactions of NO_2 and OH radicals with polycyclic aromatic hydrocarbons (PAH) adsorbed on diesel particles.[15] They concluded that the reactions with OH were approximately four orders of magnitude faster than with NO_2. Bertram et at.,[11] Molina et al.[14] and Park et al.[18] measured the reactive uptake of OH onto various organic monolayers and surfaces in a flow tube. By measuring the gas phase loss of OH they found that γ is greater than 0.1. Using a molecular beam scattering technique, Bagot et al. 2008 measured an uptake coefficient of $\gamma = 0.49 \pm 0.04$ by colliding superthermal OH radicals with a liquid squalane surface.[19]

Rather than measuring the gas phase loss of OH, the reactive uptake coefficient can be quantified by monitoring the removal of an organic molecule in the particle phase. For example, McNeill et. al. reported an uptake coefficient of ~ 0.8 – 1 by measuring the decay of palmitic acid in submicron aerosols.[10] Similarly, George et al. found a value of 1.3 ± 0.4 for the reactive uptake of OH by bis(2-ethylhexyl) sebacate (BES) particles.[9] OH concentrations in these experiments were in the range of 10^9 to 10^{11} molec·cm^{-3} and the reaction times were on the order of a few minutes. Lambe et al. used a smog chamber to study the OH oxidation of hexacosane

particles at low OH concentrations (4 – 8 x 10^6 molec·cm^{-3}) over experimental timescales of several hours.[20] They reported a reactive uptake coefficient of 1.04 ± 0.21.

This paper outlines a new method for measuring the heterogeneous chemistry of organic aerosol particles using a continuous flow stirred tank reactor (CFSTR) at lower OH concentrations than typically used in flow tubes. The main feature of the CFSTR is that the volumetric flow entering and exiting the chamber is balanced and the contents of the chamber are well mixed to produce stable reaction conditions over many hours, even days. The CFSTR has been previously used to study aerosol formation[21-23] as well as gas phase reactions.[24, 25] Fewer studies have applied CFSTR's to heterogeneous reactions on aerosol particles.[26, 27] In these previous studies, the rate of a heterogeneous or homogeneous reaction inside a CFSTR was obtained by measuring the difference between the reactant concentrations entering and exiting the reaction volume divided by the residence time, once the CFSTR has reached steady state.[26, 27]

In this paper, the photochemical evolution of aerosol particles within a CFSTR is studied in real time by monitoring the removal of particle phase reactant molecules. The mathematical framework needed to quantify the heterogeneous kinetics is developed and applied to the oxidative aging of squalane aerosol by OH in the presence of O_2. Squalane ($C_{30}H_{62}$) is a saturated branched alkane and a good proxy for long chain molecules often found in ambient aerosol particles. In addition, squalane particles are liquid at room temperature and thus spherical, which simplifies the reactive uptake coefficient analysis. By monitoring the particle-phase chemical composition as a function of reaction time using a vacuum ultraviolet time-of-flight aerosol mass spectrometer (VUV-AMS), the reactive uptake coefficient of OH by squalane particles is measured at OH concentrations of 1 – 7 x 10^8 molec·cm^{-3}. Furthermore, a general analytical expression is formulated to describe the real time sequential evolution of particle-

phase reaction products in the CFSTR that are formed by the heterogeneous reaction of squalane by OH in the presence of O_2.

II. EXPERIMENTAL SETUP

The experimental setup is shown in Fig. 1. The apparatus includes a particle generation system, a CFSTR, and an instrumental analysis system. Squalane particles are generated via homogeneous nucleation by passing 0.35 slm (standard liter per minute) of N_2 gas through a Pyrex tube containing squalane (Acros Organics, 99%) housed inside a cylindrical oven (Carbolite). The oven temperature is fixed at 125°C but can be adjusted to control the particle number and mean size. The particle flow is then passed through an activated charcoal filter to remove any residual gas phase organic compounds that may be produced in the oven. The relative humidity of the flow is fixed at 30% by mixing it with 0.3 slm of N_2 which has passed through a water bubbler. Additional flows of 0.285 slm dry N_2, 0.05 slm O_2 and 0.015 slm hexane (5 ppm in N_2) are also added, yielding a total flow rate of 1 slm into the CFSTR. The final concentration of hexane entering the CFSTR is ~75-125 ppb. Here hexane is used to determine the OH concentration using a relative rate method described below.

The 1 slm humidified flow is introduced into a Teflon-lined, ~150 L, stainless-steel chamber through a diffuser mounted on an inlet (0.635 cm in diameter) located at the top of the chamber. This CFSTR operates at atmospheric pressure and room temperature (25°C). A stainless steel impeller, located at the bottom of the chamber, ensures that the particles and gases are well-mixed once they enter the chamber. Inside the chamber two 22.86 cm long mercury Pen-ray (UVP LLC.) lamps, housed inside 2.54 cm diameter GE type 214 quartz tubes, are used for the photochemical production of OH from the photolysis of O_3 in the presence of water. The

lamps are covered with an additional GE type 219 quartz sleeve to filter out wavelengths < 220 nm. For the experiments reported here, ozone is not introduced directly into the CFSTR, but rather produced *in situ*. This is done by introducing a small gap (1.5 – 5.1 mm) in the GE type 219 quartz filter to allow a fraction of the 185 nm light produced by the lamp to enter the reactor. The 185 nm light dissociates O_2 into oxygen atoms, which in turn react with O_2 to produce ozone. O_3 is subsequently photolyzed by the primary 254 nm output of the lamps to produce $O(^1D)$ which reacts with water to form OH. Some OH can also be produced by the direct photolysis of H_2O at 185 nm. By adjusting the width of the gap in the GE type 219 filter, the amount of O_3 produced can be controlled, thus varying the average OH concentration in the chamber. The spatially averaged [OH] inside the reactor remains constant since the UV light, $[O_2]$ and relative humidity in the CFSTR remain constant during the reaction.

The experiment consists of two parts: (1) the fill and (2) reaction steps. In order to quantify the heterogeneous kinetics of OH with squalane, first the fill kinetics of the CFSTR is measured in the absence of chemistry. To do this the CFSTR is purged with N_2 (~ 5 slm) for a few hours to eliminate residual particles and hexane from the previous reaction. The empty chamber is then filled with hexane and squalane with the UV lamps off. This step is critical for quantifying the fill kinetics as detailed in section IIIA. After the filling period, which usually takes ~ 2-3 hr, the UV lamps are turned on to initiate the reaction where both the heterogeneous chemistry and the flow dynamics govern the temporal evolution of reactants and products in the CFSTR as detailed in section IIIB.

The 1 slm flow exits the CFSTR at the bottom of the chamber and is directed to three instruments: a gas chromatograph with a flame ionization detector (GC-FID, SRI 8610C) for OH quantification, a scanning mobility particle sizer (SMPS, TSI 3936) for obtaining the particle

size distribution, and a VUV-AMS for chemical analysis of the particles. To remove O_3 from the flow, a denuder (Carulite) is placed in front of the SMPS and AMS. O_3 is removed prior to the GC measurement using a separate chemical potassium iodide (KI) filter.

Particle size distributions are monitored using a SMPS system, which consists of a differential mobility analyzer (DMA, TSI 3081) and a condensation particle counter (CPC, TSI 3772). The ratio of sheath to sample flow rates in the DMA is 10:1. Before each experiment the aerosol flow is directed around the CFSTR and sent directly to the SMPS to confirm that the particle size distribution and number density of the aerosol particles emanating from the nucleator is stable before starting to fill the chamber with particles. At the end of the filling step, the mean surface area-weighted particle size exiting the chamber is typically ~ 220 ± 20 nm.

OH is quantified using a relative rate technique similar to the methods described in previous publications.[15, 29, 30] The OH concentration is computed from the time dependent decay of hexane, which is monitored by the GC-FID. For this measurement, the outflow of hexane is pre-concentrated in a Tenax^{TM}-GR adsorbent trap for 3 minutes after which hexane is thermally desorbed and injected onto the GC column. This pre-concentration step improves the detection limit of the GC to allow the use of small amounts of hexane (~ 75-125 ppb) to avoid possible interferences with the main reaction of particles with OH. Hexane is chosen as the reference compound since its rate coefficient with OH is well known[29, 31, 32] and the GC-FID responds well to this hydrocarbon.

The composition of condensed-phase squalane and its reaction products are measured using the VUV-AMS located at the Chemical Dynamics Beamline (Beamline 9.0.2) at the Advanced Light Source (ALS) (Lawrence Berkeley National Laboratory, Berkeley, CA). In this

AMS the particles are thermally vaporized at ~100°C after which the chemical composition is measured using vacuum ultraviolet (VUV) photoionization mass spectrometry. A detailed description of the AMS can be found elsewhere.[33] Unlike 70 eV electron impact ionization where many small fragments are formed when squalane is ionized, VUV photoionization preserves the molecular ion peaks in the mass spectra. Fig. 2 shows the 10.5 eV photoionization mass spectra of squalane particles before and after reaction with OH. For the kinetic measurements, detailed later, the decay of squalane (Sq) within the particles is monitored as a function of reaction time using the *m/z* = 422 molecular ion peak. As an additional check of possible interferences in the mass spectra, the largest squalane fragment ion at *m/z* = 238 is also monitored to obtain the decay kinetics. It is found that both the squalane fragment peak and the parent molecular ion (m/z = 422) yield equivalent results. Shown in Fig. 2 are the first three oxidation products, which correspond to the addition of 1, 2 and 3 oxygenated functional groups to squalane and are denoted SqO, SqO_2, and SqO_3, respectively. These oxidation products are monitored as a function of reaction time using the molecular ion peaks at *m/z* = 436, 450 and 464, respectively. A thorough analysis of the squalane oxidation kinetics, products and their chemical evolution at high OH concentration can be found in Smith et al.[28]

III. RESULTS AND DISCUSSION

A. Fill Kinetics in a CFSTR

The mathematics that describe the behavior of the CFSTR are well established.[34] The time dependent change in particle concentration (i.e. squalane) in a CFSTR in the absence of a chemical reaction is:

$$\frac{d[Sq]}{dt} = \frac{F \cdot C_{Sq}}{V} - \frac{F \cdot [Sq]}{V} - k_w^{Sq} \cdot [Sq] \quad (1)$$

where F is the flow rate entering and exiting the chamber (1 slm). C_{Sq} is the spatially averaged concentration of squalane (i.e. squalane molecules per volume of gas) at the entrance inlet, V is the chamber's volume (~150 L), t is the filling time (sec) and [Sq] is the concentration of squalane (squalane molecules per volume of gas) inside the chamber. k_w^{Sq} is the first order wall loss rate coefficient (sec^{-1}).[23] It is important to distinguish C_{Sq} from [Sq]. C_{Sq} is the particle-phase squalane concentration in the flow entering the chamber and is therefore constant. Conversely, [Sq] is the particle-phase squalane concentration inside the chamber, which is time dependent. In Eq. (1), the first term represents the concentration of squalane entering the chamber, the second term refers to the concentration of squalane exiting the reactor while the last term accounts for particle loss to the chamber wall. Solving Eq (1) for the particle-phase squalane concentration as a function of fill time ($[Sq]_{fill}$) yields,

$$[Sq]_{fill} = \frac{F \cdot C_{Sq}}{V \cdot k_f^{Sq}} - \frac{F \cdot C_{Sq}}{V \cdot k_f^{Sq}} \cdot \exp(-k_f^{Sq} \cdot t) \quad (2)$$

where $k_f^{Sq} = k_w^{Sq} + F/V$ is the rate constant for the particle filling process. An equivalent expression for the time dependent change of gas-phase hexane concentration during the filling process ($[Hex]_{fill}$) can also be derived using the same approach:

$$[Hex]_{fill} = \frac{F \cdot C_{hex}}{V \cdot k_f^{hex}} - \frac{F \cdot C_{hex}}{V \cdot k_f^{hex}} \cdot \exp(-k_f^{hex} \cdot t) \quad (3)$$

where the terms in Eq. (3) are defined in a similar way to those shown in Eq. (2). It is important to note that the squalane aerosol and hexane have different wall loss rate coefficients, therefore their filling rate constants (k_f^{Sq} and k_f^{hex}) are different and must be determined independently.

According to Eqs. (2) and (3), it would take ~15 hr under our conditions (F = 1 slm) for the particle and hexane concentrations exiting the CFSTR to reach 99.9% of the inlet concentration. However, it is not necessary to wait until the reactor is full (i.e. the squalane and hexane concentrations entering and exiting the reactor, respectively, are equal) before starting the reaction. This is because the most important quantities to be determined during the fill phase are k_f^{Sq} and k_f^{hex}. As seen in Eqs. (2) and (3), k_f^{Sq} and k_f^{hex} appear in the amplitude, offset and rate constant of the exponential function and thus in principle can be determined in three different ways. For example, Guo and Kamens described a similar CFSTR method where they, in effect, obtained the rate coefficients using the offset in Eq. (2).[26] To reliably determine k_f in this way requires the concentrations in the CFSTR to reach steady state which can take many hours. Similarly, obtaining the fill rate constants from the amplitude of the exponential in Eq. (2) also requires long equilibration times for a large chamber. Moreover, obtaining fill rate coefficients using the amplitude or offset requires reliable and precise measurements of the absolute values of F, C_{Sq}, C_{hex}, and V, which may not always be possible. Furthermore, uncertainties in the absolute concentrations of hexane or squalane, the chamber volume or flow rate all translate into substantial errors in determining k_f.

For these reasons, it was found that the simplest and most accurate way to extract k_f^{Sq} and k_f^{hex} is from the rate constant in the exponential fitting function. Fig. 3 shows the increase in the hexane peak area (measured by the GC) and squalane mass concentration (measured by the

SMPS) as a function of fill time, starting with an empty reactor. For convenience, the SMPS is used to monitor the change in particle mass (using the density of squalane: 0.8 g·cm^{-3}) in the CFSTR during the fill period instead of the VUV-AMS. Previous checks confirmed that the un-reacted squalane ion signal (m/z = 422) in the VUV-AMS is proportional to the total volume distribution measured by the SMPS, so that the fill kinetics can be measured with either device. The data, shown in Fig. 3, are fit to the exponential form represented by Eqs. (2) and (3). k_f^{Sq} and k_f^{hex} are then obtained directly from the rate constant via the exponential fit. Although the [Sq] and [Hex] are only within 90% of C_{Sq} and C_{hex} after 2-3 hours of filling at 1 slm rate, it is found that 2-3 hours provides ample fill data for the accurate determination of k_f^{Sq} and k_f^{hex} using this method. Furthermore, the exponential rise of the hexane and squalane concentrations observed in Fig. 3 provides a clear signature that the reactor chamber is well-mixed and thus the outflow has the same composition as the contents of the chamber. Therefore, the CFSTR described here can be reliably modeled as an idealized mixed flow reactor using Eq. (1). This was further confirmed by turning off the impeller, which resulted in poor mixing and non-exponential hexane and squalane fill kinetics.

B. Heterogeneous Reactions in a CFSTR

After a satisfactory filling time (~ 2 – 3 hr), both UV lamps are turned on to initiate the chemical reaction. The initial concentrations of hexane $[Hex]_0$, measured by the GC, and squalane $[Sq]_0$, measured by the VUV-AMS at *m/z* = 422, are recorded moments before the lamps are turned on to start the reaction. OH radicals are produced nearly instantaneously from the photolysis of O_3 in the presence of H_2O vapor, thus starting the reaction with the squalane aerosol as well as the gas phase tracer hexane. The subsequent analysis assumes that during the

course of the reaction squalane and hexane are both exposed to the same uniform OH concentration in the chamber. The validity of this assumption will be evaluated later. The time dependent decay of hexane due to the reaction with OH is,

$$\frac{d[Hex]}{dt} = -k_{hex} \cdot [OH] \cdot [Hex] = -k'_{hex} \cdot [Hex], \quad (4)$$

where [Hex] and [OH] are the concentrations of hexane and OH (molec·cm^{-3}) in the chamber, respectively. t is the reaction time (sec) and k_{hex} is the second order rate constant (cm^3·molec^{-1} ·sec^{-1}). Assuming that [OH] is constant, the time evolution of hexane can be expressed as a pseudo-first order reaction where k'_{hex} is the pseudo-first order rate constant (sec^{-1}).

If molecules within a particle are well-mixed, then the fraction of squalane within the surface region of the particle is equivalent to that of the bulk. Previously, we examined the reaction of squalane + OH under flow tube conditions (high OH concentration and short reaction time) and found strong evidence that the particles were indeed well mixed.[28] Therefore, an expression equivalent to Eq. (4) can be written for the reaction of OH with the squalane aerosol.

$$\frac{d[Sq]}{dt} = -k_{Sq} \cdot [OH] \cdot [Sq] = -k'_{Sq} \cdot [Sq] \quad (5)$$

The time evolution of the spatially averaged [Sq] concentration (molec·cm^{-3}) can be written as a pseudo-first order reaction similar to hexane, where k_{Sq} is the second order rate constant (cm^3·molec^{-1}·sec^{-1}) and $k'_{Sq} = k_{Sq}[OH]$ and represents the pseudo-first order rate constant (sec^{-1}). k_{Sq} is a heterogeneous rate coefficient and its relationship to the reactive uptake coefficient, γ, is shown later in Eq. (11).

Eqs. (4) and (5) alone are insufficient to describe the temporal behavior of squalane and hexane in the CFSTR. This is because in addition to the chemical decay there is the continual flow of squalane and hexane in and out of the chamber during the course of the reaction. To account for these factors, Eq. (5) is incorporated into Eq. (1) to describe the heterogeneous chemistry as well as the flow dynamics of the CFSTR to obtain:

$$\frac{d[Sq]}{dt} = \frac{F \cdot C_{Sq}}{V} - \frac{F \cdot [Sq]}{V} - k_w^{Sq} \cdot [Sq] - k'_{Sq} \cdot [Sq] \qquad (6)$$

This equation is similar to Eq. (1) except for the last term that accounts for the heterogeneous loss of squalane due to reaction with OH. Eq. (6) can be integrated to find the time evolution of squalane normalized to its initial concentration ($[Sq]_0$) :

$$\frac{[Sq]}{[Sq]_0} = \frac{F \cdot C_{Sq}}{V \cdot [Sq]_0 \cdot (k_f^{Sq} + k'_{Sq})} + \left[1 - \frac{F \cdot C_{Sq}}{V \cdot [Sq]_0 \cdot (k_f^{Sq} + k'_{Sq})}\right] \cdot \exp\left[-\left(k_f^{Sq} + k'_{Sq}\right) \cdot t\right] \qquad (7)$$

The time evolution of the normalized hexane signal can also be found using the same approach:

$$\frac{[Hex]}{[Hex]_0} = \frac{F \cdot C_{hex}}{V \cdot [Hex]_0 \cdot (k_f^{hex} + k'_{hex})} + \left[1 - \frac{F \cdot C_{hex}}{V \cdot [Hex]_0 \cdot (k_f^{hex} + k'_{hex})}\right] \cdot \exp\left[-\left(k_f^{hex} + k'_{hex}\right) \cdot t\right] \qquad (8)$$

Eqs. (7) and (8) have the same functional form for the time evolution of both hexane and squalane in the CFSTR. At first glance this might seem surprising since OH reacts *heterogeneously* with squalane and *homogeneously* with gas phase hexane. Levenspiel[35] explicitly considered this and derived the reaction rate and product conversion expressions for a variety of reactor types when suspended aggregates (i.e. aerosols) are present in the reactor volume. The "degree of aggregation" (e.g. aerosols) was found not to change the expression for the reaction rate and product conversion in idealized batch and plug flow reactors. In this case,

heterogeneous reactions are treated mathematically in the same way as a homogeneous reaction in a gas or liquid. This is because each small aggregate or particle can be treated, in essence, as a tiny idealized batch reactor. He found for mixed flow reactors, such as the CFSTR described here, that this is not necessarily true and in some cases the "degree of aggregation" leads to a different mathematical expression for the reaction rate in a CFSTR. However, as shown by Levelspiel,[35] first order reactions involving aggregates in a CFSTR are a special case and can be treated in the same way as a first order homogeneous gas or liquid phase reactions as is done here. This mathematical equivalence, however, does not necessarily hold for zero or second order reactions for example. Since [OH] is constant and the particle phase is well-mixed, the rate of reaction can be expressed as pseudo-first order with respect to squalane. This in turn yields an overall expression for the evolution of squalane in a CFSTR that is equivalent in form to that of gas phase hexane. A similar analysis was used by Guo and Kamens to measure the heterogeneous photoxidation of particle bound polycyclic aromatic hydrocarbons in a CFSTR.[26, 27]

Fig. 4 shows the decay of squalane and hexane during the reaction period each fit to the offset exponential decay of the form shown in Eqs. (7) and (8). Squalane and hexane do not decay to zero but rather approach a constant value that reflects the characteristic of the continuous flow operation, in which new squalane and hexane are continually introduced into the CFSTR during the reaction. In Eqs. (7) and (8), the exponential decay constant is the sum of k_f^{Sq} and k'_{Sq} for squalane, and k_f^{hex} and k'_{hex} for hexane. Therefore, both k'_{Sq} and k'_{hex} can be obtained from the exponential decay data, shown in Fig. 4, since the fill rate constants (k_f^{Sq} and k_f^{hex}) were measured before the reaction as described in IIIA. From the relationship $k'_{hex} = k_{hex}\cdot[OH]$,

the OH concentration can be computed using the hexane + OH rate constant (k_{hex} = 5.20 x 10^{-12} $cm^3 \cdot molec^{-1} \cdot sec^{-1}$) as reported by Atkinson et al.[32] After the [OH] is determined from the hexane decay, k_{Sq} can be directly computed from $k_{Sq} = k'_{Sq}[OH]^{-1}$.

As a check of the overall method and assumptions described above a test experiment is conducted to measure the rate constant (k_{but}) for the n-butane + OH reaction. The experimental setup is similar to the one described above, except that butane (~ 225 ppb) is used instead of squalane aerosol. The total flow is maintained at 1 slm, consisting of 0.1 slm O_2, 0.3 slm humidified N_2, 0.54 slm N_2, 0.015 slm hexane (5 ppm in N_2) and 0.045 slm butane (5 ppm in N_2). The GC is used to measure both the fill and the decay kinetics that are shown in Fig. 5. The OH concentration, computed from the hexane decay, is found to be 2.42 x 10^8 $molec \cdot cm^{-3}$, using the value k_{hex} = 5.20 x 10^{-12} $cm^3 \cdot molec^{-1} sec^{-1}$. The method yields a value of k_{but} = (2.41 ± 0.48) x 10^{-12} $cm^3 \cdot molec^{-1} \cdot sec^{-1}$. This value is in good agreement with the value suggested by Donahue and Clarke: k_{but} = (2.54 ± 0.08) x 10^{-12} $cm^3 \cdot molec^{-1} \cdot sec^{-1}$(at 295K).[36] This result thus confirms that the overall method can be used to reliably obtain rate constants for OH oxidation reactions.

As emphasized above, the offset in the decay of squalane and hexane, shown in Figs. 4 and 5, is due to the continuous introduction of these species into the CFSTR during the reaction. Additional experiments are conducted in a slightly different mode to broadly explore the operation of the CFSTR described here. After the normal filling process, the hexane and aerosol flows into the chamber are turned off and replaced with particle free nitrogen at the start of the chemical reaction. The total flow going into the reactor is still maintained at 1 slm, containing 30% relative humidity, 0.05 slm O_2 and 0.75 slm dry N_2. By eliminating the incoming flow of

particles and hexane, the first term in Eq. (6) becomes zero and the offset in the exponential decay disappears to yield the following mathematical expression:

$$\frac{[Sq]}{[Sq]_0} = \exp\left[-\left(k_f^{Sq} + k'_{Sq}\right)\cdot t\right] \tag{9}$$

for the time evolution of squalane particles during the reaction period. The same exponential form can also be found for hexane:

$$\frac{[Hex]}{[Hex]_0} = \exp\left[-\left(k_f^{hex} + k'_{hex}\right)\cdot t\right] \tag{10}$$

Here the analytical expression for the decay of squalane and hexane is much simpler with the exponential form decaying to zero. In this case, the decay of hexane and squalane as a function of time is due both to the reaction with OH and from dilution since the incoming flow contains no hexane or squalane. This approach could be a more precise way to examine any changes in particle size during the course of the reaction without the influence of new particles entering the reactor. However, for the experiments reported here the particle size distribution measured by both approaches is found to remain constant to within 10% over the course of the reaction.

Fig. 6 shows the decay of squalane as a function of OH concentration observed during the reaction period using both experimental approaches. The results are fit using the appropriate exponential forms as outlined above. In Fig. 6(a), as expected, the rate of squalane decay increases with increasing OH concentration. In addition, the decrease in the observed offset in the squalane decay with increasing OH concentration reflects the increase in k'_{Sq} as predicted by Eq. (7). In the alternative experimental approach (Fig. 6(b)), (where squalane and hexane are

turned off during the reaction) squalane decays exponentially to 0 as predicted by Eq. (9). The second order rate constant for the reaction squalane + OH is computed from each experiment as outlined above and shown in Table 1.

Two important assumptions are made in the determination of the OH concentration. The first assumption is that OH will only react with hexane. This assumption was verified by comparing the calculated OH concentration with the modeled OH concentration using a kinetics program.[28] The model verified that 99% of the hexane is lost to the reaction with OH. The second assumption is that the OH concentration in the reactor is uniform. This may or may not be the case because the OH concentration is likely to be higher near the UV lamps where the ozone photolysis rate is the highest. The distribution of OH radicals within the ~150L chamber volume therefore may not be perfectly uniform. However, it is likely that the spatially *averaged* OH concentration inside the chamber remains constant throughout the course of an experiment since the relative humidity, O_2 and lamp power are fixed during the reaction. With the particles and hexane well mixed inside the reactor, on average, the particles and hexane exiting the reactor will both sample the same constant average OH concentration over the course of the reaction. This average OH concentration therefore can be taken to be approximately equivalent to a uniform OH distribution inside the reactor. The test with n-butane described above provides further evidence that any non-uniformity in the OH distribution inside the CFSTR does not lead to large errors in the calculation of the reaction rate coefficients reported here.

C. Determination of the Reactive Uptake Coefficient

The reactive uptake coefficient (γ) for the OH oxidation of squalane particles, in the presence of O_2, can now be determined from the second order rate coefficients k_{Sq} shown in

Table 1. Here we use the formulation of the reactive uptake coefficient reported by Smith et al.,[28] where γ is defined as the fraction of OH collisions with squalane in the particle that lead to reaction.

$$\gamma = \frac{4 \cdot k_{Sq} \cdot D \cdot \rho_0 \cdot N_A}{\bar{c} \cdot 6 \cdot M_{Sq}} \tag{11}$$

where D is the mean surface area-weighted particle diameter obtained from the SMPS, ρ_0 is the initial squalane particle-phase density (ρ_0 = 0.8 g·cm^{-3}), N_A is Avogadro's number, $\bar{c}$ is the mean speed of OH molecules and M_{Sq} is the molar mass of squalane (422 g/mole). Eq. (11) assumes that the squalane in the particles is consumed only by the reaction with OH and that the loss rate of gas phase OH is equal to the loss rate of squalane. The particle density is assumed to be constant during the reaction and taken to be that of squalane (0.8 g/cm^3). Volatilization is also neglected since it was found that over the OH concentration used here the particle diameter remains constant during the course of the reaction with an average value of D = 220 ± 20 nm.

Table 1 shows the calculated values of γ, obtained from the data shown in Fig. 6, using Eq. (11). The average reactive uptake coefficient computed from these measurements is 0.51 ± 0.02 where the stated error represents one standard deviation calculated from the five seperate measurements of gamma shown in Table 1. This error does not include uncertainties in the OH concentration. To account for these we use the 20% uncertainty in the rate constant (k_{hex}) of n-hexane + OH as reported by Atkinson et al.[32] to obtain γ = 0.51 ± 0.10. Due to unknown amounts of secondary chemistry,[39] the reactive uptake coefficient reported here is not corrected for gas-phase diffusion.

D. The Formation of Oxidation Products in a CFSTR

In addition to the decay of squalane, oxidation products are formed and evolve over the course of the reaction in the CFSTR. Figs. 7 and 8 show the squalane decay and the evolution of the first three oxidation products using both experimental approaches (with and without offset as explained above). The products are monitored using the three peaks with the strongest signals in the product spectra: *m/z* = 436 (SqO) and *m/z* = 450 (SqO_2), and *m/z* = 464 (SqO_3), which correspond to the addition of one, two and three oxygenated functional groups to squalane, respectively.[28] The ion signals are normalized to account for any changes in the photon flux.

The general mechanism for the reaction of OH with gas-phase hydrocarbons (including simple organic aerosols) has been proposed previously.[9, 14, 37, 38] The reaction is initiated by OH abstracting a hydrogen atom from a hydrocarbon, in this case squalane, producing H_2O and an alkyl radical. The alkyl radical then reacts rapidly in the presence of O_2 to form an alkyl peroxy radical intermediate, which can further react via a number of different pathways (self-reaction, reaction with HO_2, isomerization, etc) to eventually form stable oxygenated products, which could include hydroperoxides, alcohols, ketones, etc

It was shown recently by Smith et al.[28] that for the squalane + OH reaction at high OH concentrations ([OH] ~ 1 x 10^{10} molec·cm^{-3}) the stable oxygenated reaction products evolve via the sequential addition of 1 oxygenated functional group per reactive loss of squalane. It was also found that a simple oxidation model in which squalane and its oxidation products reacted with OH with the same second order rate coefficient could explain the chemical evolution of the particles as a function of OH exposure (i.e. [OH]·time) in the flow tube reactor. This generalized mechanism for the reaction squalane + OH in the presence of O_2 can be written as[28]:

$$\mathrm{Sq} + \mathrm{OH} \xrightarrow[\mathrm{O_2}]{\mathrm{k_{Sq}}} \mathrm{SqO} \tag{12}$$

$$\mathrm{SqO} + \mathrm{OH} \xrightarrow[\mathrm{O_2}]{\mathrm{k_{Sq}}} \mathrm{SqO_2} \tag{13}$$

$$\mathrm{SqO_n} + \mathrm{OH} \xrightarrow[\mathrm{O_2}]{\mathrm{k_{Sq}}} \mathrm{SqO_{n+1}} \tag{14}$$

To examine whether this sequential oxidation model correctly describes the chemistry of product formation at the lower OH concentration and longer reaction times reported here, this model is incorporated into the equations that govern the chemistry and flow dynamics of the CFSTR. The expression for the time evolution of the first oxidation product, SqO (squalane + one O atom), can be derived from a differential equation similar to squalane parent:

$$\frac{d[SqO]}{dt} = k'_{Sq} \cdot [Sq] - k'_{Sq} \cdot [SqO] - \frac{F \cdot [SqO]}{V} - k_w^{Sq} \cdot [SqO] \tag{15}$$

The first term in Eq. (15) accounts for the formation of SqO by the reaction of squalane with OH (i.e. Eq. (12)). The second term accounts for the loss of SqO to the reaction with OH to form SqO_2 as shown in Eq. (13). The last two terms account for the quantity of SqO in the flow exiting the reactor and lost to the reactor walls, respectively. This is a first-order linear differential equation and can be solved using a general method. The solution to this equation is:

$$\frac{[SqO]}{[Sq]_0} = \frac{A \cdot k'_{Sq}}{k_f^{Sq} + k'_{Sq}} + k'_{Sq} \cdot \left[t - A \cdot t - \frac{A}{k_f^{Sq} + k'_{Sq}} \right] \cdot \exp\left[-\left(k_f^{Sq} + k'_{Sq} \right) \cdot t \right] \tag{16}$$

where $A = \dfrac{F \cdot C_{Sq}}{V \cdot [Sq]_0 \cdot (k_f^{Sq} + k'_{Sq})}$.

The same process is applied to find the expressions for subsequent oxidation products. The general analytical expression for the time evolution of the oxidation products (including squalane) in a CFSTR is:

$$\frac{[SqO_n]}{[Sq]_0} = \frac{A \cdot \left(k'_{Sq}\right)^n}{\left(k_f^{Sq} + k'_{Sq}\right)^n} + \left[\frac{\left(k'_{Sq}\right)^n \cdot t^n}{n!} - \frac{A \cdot \left(k'_{Sq}\right)^n}{\left(k_f^{Sq} + k'_{Sq}\right)^n} \cdot \sum_{i=0}^{n} \frac{t^i \cdot \left(k_f^{Sq} + k'_{Sq}\right)^i}{i!} \right] \cdot \exp\left[- \left(k_f^{Sq} + k'_{Sq}\right) \cdot t \right] \quad (17)$$

$$(n = 0, 1, 2 \ldots)$$

where $[SqO_n]$ is the concentration of the n^{th} oxidation product (n = 0 refers to squalane parent). To describe the experimental data shown in Fig 7, Eq. 17 is simplified to:

$$\frac{[SqO_n]}{[Sq]_0} = B_n + \left[D_n \cdot t^n - B_n \cdot \sum_{i=0}^{n} \frac{t^i \cdot \left(k_f^{Sq} + k'_{Sq}\right)^i}{i!} \right] \cdot \exp\left[- \left(k_f^{Sq} + k'_{Sq}\right) \cdot t \right] \quad (18)$$

where B_n and D_n are adjustable parameters used in place of the terms in Eq. (17) to account for differences in VUV photoionization cross sections and fragmentation patterns of squalane and its oxidation products.

In the alternative approach, in which no hexane or squalane is introduced into the CFSTR during the reaction, the general analytical expression for squalane oxidation simplifies to:

$$\frac{[SqO_n]}{[Sq]_0} = \frac{G_n \cdot \left(k'_{Sq}\right)^n \cdot t^n}{n!} \cdot \exp\left[- \left(k_f^{Sq} + k'_{Sq}\right) \cdot t \right] \quad (19)$$

$$(n = 0, 1, 2\ldots)$$

where the adjustable parameter G_n is added to the expression to account for differences in VUV photoionization cross sections and fragmentation patterns of squalane and its oxidation products.

Using Eqs. (18) and (19) the time evolution of the first three oxidation products (SqO, SqO_2 and SqO_3) are fit by first fixing k_{Sq} to the second order rate coefficient obtained from the decay of squalane (Eq. (9)). The least squares fit of the model to the experimental data is then obtained by adjusting two parameters B_n and D_n for the exponential decay with an offset (shown in Fig. 7), or by adjusting a single parameter G_n for the exponential decay with no offset (shown in Fig. 8). With a single k_{Sq}, as assumed in the sequential oxidation model, the time evolution of the squalane parent peak and its first three oxidation products can be reproduced by the oxidation model. These results confirm that even at these lower OH concentrations the sequential oxidation model proposed by Smith et al.[28] accounts for the overall chemical transformation of the particle. This model predicts that one O atom is added per reactive loss of squalane, and that squalane reacts via the same rate coefficient as its oxidation products. This could imply that there are not significant differences in the overall chemistry occurring at high and low OH concentrations. However, as will be discussed below, the absolute rate of the heterogeneous reaction, measured via the particle phase loss of squalane, does indeed depend upon the OH concentration.

The reactive uptake coefficient ($\gamma = 0.51 \pm 0.10$) for the heterogeneous reaction of OH with squalane reported here, using a CFSTR, is well within the range, $\gamma = 0.2$ to 1, found in earlier experiments.[8-11,18] However, we previously measured a smaller reactive uptake coefficient ($\gamma = 0.3 \pm 0.07$) for the OH + squalane reaction in a flowtube system using [OH] ~ 1 x 10^{10} molec·cm^{-3}.[28] Although the sequential oxidation model correctly describes the chemical evolution of reaction products in both the flowtube and CFSTR reactors, it is found that at low [OH] the loss rate of squalane in the particle appears to accelerate. For the reactive uptake coefficient to depend on the average [OH] in this way would suggest an additional loss channel for squalane. For example, the primary heterogeneous reaction forms radical intermediates (e.g.

RO_2 and RO) that can in principle abstract a hydrogen atom from a neighboring molecule, thus opening a secondary loss channel for squalane in the particle phase. The influence that these secondary loss channels have on the measured uptake coefficient should depend upon the secondary loss rates relative to the primary OH abstraction rate. For example, at high OH concentration squalane loss may be dominated by the direct reaction with OH thereby obscuring the presence of secondary chemistry. A detailed chemical mechanism that accounts for both the secondary abstraction reactions and the potential photochemistry of reaction intermediates is currently under investigation and will be explored in a forthcoming publication.[39]

Finally, it is in principle possible to solve for the general case in which the reaction rate coefficient of the parent molecule is different than that of its subsequent oxidation products. This case might be more appropriate for systems where the parent hydrocarbon exhibits a much different reactivity towards OH than its oxidation products. The general mathematical solution for this case in the CFSTR is extremely complicated and thus is not explicitly considered at this time.

IV. CONCLUSION

Using the OH oxidation of squalane particles as a proxy, this paper demonstrates the use of a new analytical approach to quantify the reactive uptake coefficient of OH radicals on organic particles in a CFSTR. This method is a simple and reproducible way to quantify heterogeneous reactions over many hours at well-controlled OH concentrations. Although the [OH] used in this paper is still higher than that of the atmosphere, (~ 10^6 molec·cm^{-3}), in principle, lower [OH] and longer reaction times can be readily obtained. For example, lower [OH] can be reached by reducing the UV lamp power, or decreasing the relative humidity inside

the reactor. Longer reaction times can be achieved by reducing the flow rate (F) or by using a larger volume CFSTR to obtain the desired oxidation conditions.

The general analytical solution for the time-dependent evolution of both parent and squalane oxidation products in the particles are derived. The results found here support our earlier sequential oxidation model in which one oxygenated functional group is added per the reactive loss of squalane. We again verify that the reaction of subsequent oxidation products with OH, within our experimental error, can be described by the same rate coefficient as that of main squalane + OH reaction.

Acknowledgements.

This work was supported by the Director, Office of Energy Research, Office of Basic Energy Sciences, Chemical Sciences Division of the U.S. Department of Energy under Contract No. DE-AC02-05CH11231. J.D.S is supported by the Camille and Henry Dreyfus foundation postdoctoral program in environmental chemistry. D.L.C. is grateful to the National Aeronautics and Space Administration for support on Grant NASA-NNG06GGF26G. S.R.L acknowledges the support of a Morris Belkin Visiting Professorship at the Weizmann Institute of Science. The authors wish to acknowledge the technical contributions of Drs. Christophe Nicolas (SOLEIL) and Erin Mysak (LBNL) to the construction of the CFSTR.

V. REFERENCES

1. M. Kanakidou, J. H. Seinfeld, S. N. Pandis, I. Barnes, F. J. Dentener, M. C. Facchini, R. Van Dingenen, B. Ervens, A. Nenes, C. J. Nielsen, E. Swietlicki, J. P. Putaud, Y. Balkanski, S. Fuzzi, J. Horth, G. K. Moortgat, R. Winterhalter, C. E. L. Myhre, K. Tsigaridis, E. Vignati, E. G. Stephanou and J. Wilson, *Atmospheric Chemistry and Physics*, 2005, **5**, 1053-1123.
2. A. H. Goldstein and I. E. Galbally, *Environmental Science & Technology*, 2007, **41**, 1514-1521.
3. D. Y. Kim and V. Ramanathan, *Journal of Geophysical Research-Atmospheres*, 2008, **113**.
4. G. B. Ellison, A. F. Tuck and V. Vaida, *Journal of Geophysical Research-Atmospheres*, 1999, **104**, 11633-11641.
5. Y. Rudich, *Chemical Reviews*, 2003, **103**, 5097-5124.
6. M. C. Jacobson, H. C. Hansson, K. J. Noone and R. J. Charlson, *Reviews of Geophysics*, 2000, **38**, 267-294.
7. U. Poschl, *Angewandte Chemie-International Edition*, 2005, **44**, 7520-7540.
8. P. L. Cooper and J. P. D. Abbatt, *Journal of Physical Chemistry*, 1996, **100**, 2249-2254.
9. I. J. George, A. Vlasenko, J. G. Slowik, K. Broekhuizen and J. P. D. Abbatt, *Atmospheric Chemistry and Physics*, 2007, **7**, 4187-4201.
10. V. F. McNeill, R. L. N. Yatavelli, J. A. Thornton, C. B. Stipe and O. Landgrebe, *Atmos. Chem. Phys. Discuss.*, 2008, **8**.
11. A. K. Bertram, A. V. Ivanov, M. Hunter, L. T. Molina and M. J. Molina, *Journal of Physical Chemistry A*, 2001, **105**, 9415-9421.
12. Y. Katrib, G. Biskos, P. R. Buseck, P. Davidovits, J. T. Jayne, M. Mochida, M. E. Wise, D. R. Worsnop and S. T. Martin, *Journal of Physical Chemistry A*, 2005, **109**, 10910-10919.
13. J. D. Hearn and G. D. Smith, *Journal of Physical Chemistry A*, 2004, **108**, 10019-10029.

14. M. J. Molina, A. V. Ivanov, S. Trakhtenberg and L. T. Molina, *Geophysical Research Letters*, 2004, **31**.

15. W. Esteve, H. Budzinski and E. Villenave, *Atmospheric Environment*, 2006, **40**, 201-211.

16. Y. Rudich, N. M. Donahue and T. F. Mentel, *Annual Review of Physical Chemistry*, 2007, **58**, 321-352.

17. R. G. Prinn, J. Huang, R. F. Weiss, D. M. Cunnold, P. J. Fraser, P. G. Simmonds, A. McCulloch, C. Harth, S. Reimann, P. Salameh, S. O'Doherty, R. H. J. Wang, L. W. Porter, B. R. Miller and P. B. Krummel, *Geophysical Research Letters*, 2005, **32**.

18. J. H. Park, A. V. Ivanov and M. J. Molina, *Journal of Physical Chemistry A*, 2008, **112**, 6968-6977.

19. P. A. J. Bagot, C. Waring, M. L. Costen and K. G. McKendrick, *Journal of Physical Chemistry C*, 2008, **112**, 10868-10877.

20. A. T. Lambe, J. Y. Zhang, A. M. Sage and N. M. Donahue, *Environmental Science & Technology*, 2007, **41**, 2357-2363.

21. J. E. Shilling, Q. Chen, S. M. King, T. Rosenoern, J. H. Kroll, D. R. Worsnop, K. A. McKinney and S. T. Martin, *Atmospheric Chemistry and Physics*, 2008, **8**, 2073-2088.

22. J. G. Crump and J. H. Seinfeld, *Aiche Journal*, 1980, **26**, 610-616.

23. J. H. Seinfeld, T. E. Kleindienst, E. O. Edney and J. B. Cohen, *Aerosol Science and Technology*, 2003, **37**, 728-734.

24. M. W. Gery, D. L. Fox, R. M. Kamens and L. Stockburger, *Environmental Science & Technology*, 1987, **21**, 339-348.

25. M. W. Gery, D. L. Fox, H. E. Jeffries, L. Stockburger and W. S. Weathers, *International Journal of Chemical Kinetics*, 1985, **17**, 931-955.

26. Z. Guo and R. M. Kamens, *Journal of Atmospheric Chemistry*, 1991, **12**, 137-151.

27. Z. Guo, University of North Carolina at Chapel Hill, 1987.

28. J. D. Smith, Kroll, J. H., Cappa, C. D., Che, D. L., Liu, C. L., Ahmed, M., Leone, S R., Worsnop, D. R., and Wilson, K. R., *Atmos. Chem. Phys. Discuss.*, 2009, **9**, 3945-3981.

29. W. B. DeMore and K. D. Bayes, *Journal of Physical Chemistry A*, 1999, **103**, 2649-2654.

30. E. W. Wilson, W. A. Hamilton, H. R. Mount and W. B. DeMore, *Journal of Physical Chemistry A*, 2007, **111**, 1610-1617.

31. N. M. Donahue, J. G. Anderson and K. L. Demerjian, *Journal of Physical Chemistry A*, 1998, **102**, 3121-3126.

32. R. Atkinson, *Atmospheric Chemistry and Physics*, 2003, **3**, 2233-2307.

33. K. R. Wilson, M. Jimenez-Cruz, C. Nicolas, L. Belau, S. R. Leonet and M. Ahmed, *Journal of Physical Chemistry A*, 2006, **110**, 2106-2113.

34. D. R. Mason and E. L. Piret, *Industrial and Engineering Chemistry*, 1950, **42**, 817-825.

35. O. Levenspiel, *Chemical Reaction Engineering*, 3rd edn., John Wiley & Sons, New Jersey, 1999.

36. N. M. Donahue and J. S. Clarke, *International Journal of Chemical Kinetics*, 2004, **36**, 259-272.

37. R. Atkinson, *Journal of Physical and Chemical Reference Data*, 1997, **26**, 215-290.

38. T. L. Eliason, J. B. Gilman and V. Vaida, *Atmospheric Environment*, 2004, **38**, 1367-1378.

39. J. D. Smith, C. D. Cappa, D. L. Che, C. Liu, M. Ahmed, S. R. Leone, K. R. Wilson, unpublished work.

Table 1. **Reactive uptake coefficients and second order rate coefficients as a function of OH concentration.** The experiments are conducted under normal conditions (with an offset in the decay) except for the first value (*), which is obtained using the alternative method with no offset (as described in the text).

[OH] (molec·cm^{-3})	k_{Sq} (cm^3·molec^{-1}·s^{-1})	Uptake coefficient
1.19 x 10^{8*}	1.85 x 10^{-12}	0.54
1.93 x 10^8	1.76 x 10^{-12}	0.52
2.93 x 10^8	1.79 x 10^{-12}	0.49
4.23 x 10^8	1.78 x 10^{-12}	0.51
6.87 x 10^8	1.96 x 10^{-12}	0.51

Fig. 1. Experimental apparatus used to study the heterogeneous oxidation of organic aerosols using the CFSTR.

Fig. 2. 10.5 eV photoionization mass spectra of squalane particles **(a)** before and **(b)** after reaction with [OH] = 6.78×10^8 molec·cm^{-3} for 25 min. Upon reaction there is a decrease in the squalane (Sq) peak intensity and the appearance of oxidation product peaks (SqO, SqO_2 , SqO_3). (c) An expanded view of mass spectrum showing the oxidation products.

Fig. 3. The time evolution of **(a)** hexane (measured by the GC) and **(b)** squalane (measured by the SMPS) during the filling stage of the CFSTR. The SMPS volume concentration is converted into a mass concentration using a density of 0.8 g/cm^3. The data are fit (solid lines) using Eq. (2) for squalane and Eq. (3) for hexane.

Fig. 4. Normalized concentration of **(a)** hexane (GC) and **(b)** squalane (VUV-AMS) as a function of reaction time with [OH] = 1.93×10^8molec·cm^{-3}. The data are fit (solid lines) using the exponential form with an offset shown in Eq. (7) for squalane and Eq. (8) for hexane.

Fig. 5. Experimental determination of the n-butane + OH reaction rate coefficient using hexane as a reference compound: **(a)** the time evolution of the hexane (▲) and butane (●) GC peak areas during the filling process. **(b)** The normalized decay of hexane (▲) and butane (●) as a function of reaction time at [OH] = 2.42×10^8molec·cm^{-3}. The data are fit (dashed lines for hexane and solid lines for butane) using Eq. (3) for the filling process and Eq. (4) for the reaction process.

Fig. 6. (a) Normalized squalane decays as function of reaction time for (○) [OH] = 1.93×10^8 molec·cm^{-3}, (■) [OH] = 2.93×10^8 molec·cm^{-3}, (Δ) [OH] = 4.23×10^8 molec·cm^{-3} and (●) [OH] = 6.87×10^8 molec·cm^{-3}. Squalane decays are measured using the first experimental approach in which the hexane and particles are continuously sent into the CFSTR during the reaction. Solid

lines are fits to the data using Eq. (7). **(b)** (□) [OH] = 1.19 x 10^8 molec·cm^{-3}. Squalane decay measured using the alternative experimental approach in which hexane and particles flows were turned off during the reaction. The solid line is an exponential fit to the data using the in Eq. (9).

Fig. 7. Time evolution of (a) squalane and its' first three oxidation products: (b) SqO, (c) SqO_2, (d) SqO_3 upon exposure to [OH] = 1.93 x 10^8 molec·cm^{-3} (with offset in the decays as described in text). Solid lines are fits using the general product evolution form shown in Eq. (18).

Fig. 8. The time evolution of (a) squalane and its' first three oxidation products (b) SqO, (c) SqO_2, (d) SqO_3 upon exposure to [OH] = 1.19 x 10^8 molec·cm^{-3} (with no offset in the decays as described in the text). Solid lines are fits to the data using the general product evolution expression shown in Eq. (19).

Fig. 1.

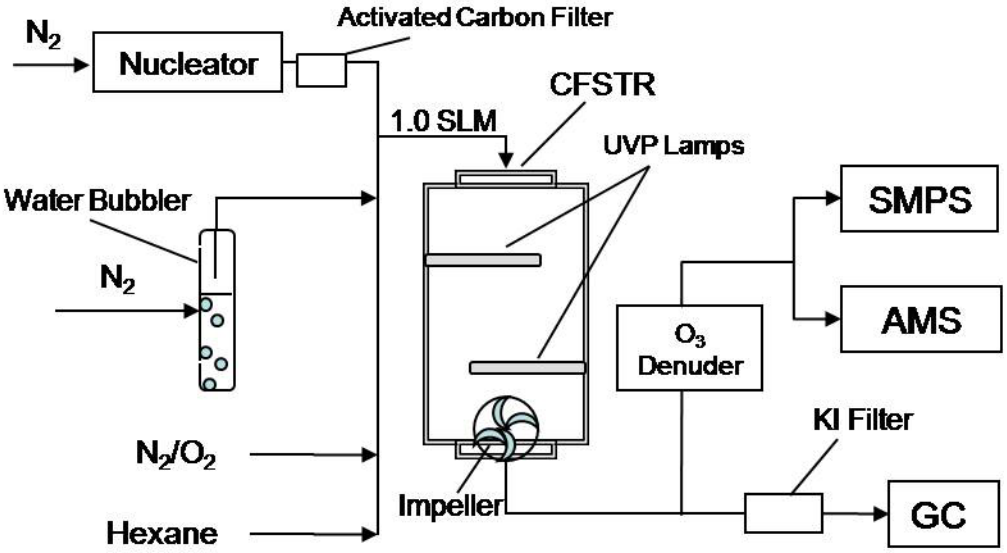
N_2
Nucleator
Activated Carbon Filter
CFSTR
1.0 SLM
UVP Lamps
Water Bubbler
N_2
SMPS
AMS
O_3 Denuder
KI Filter
N_2/O_2
Impeller
GC
Hexane

Fig. 2.

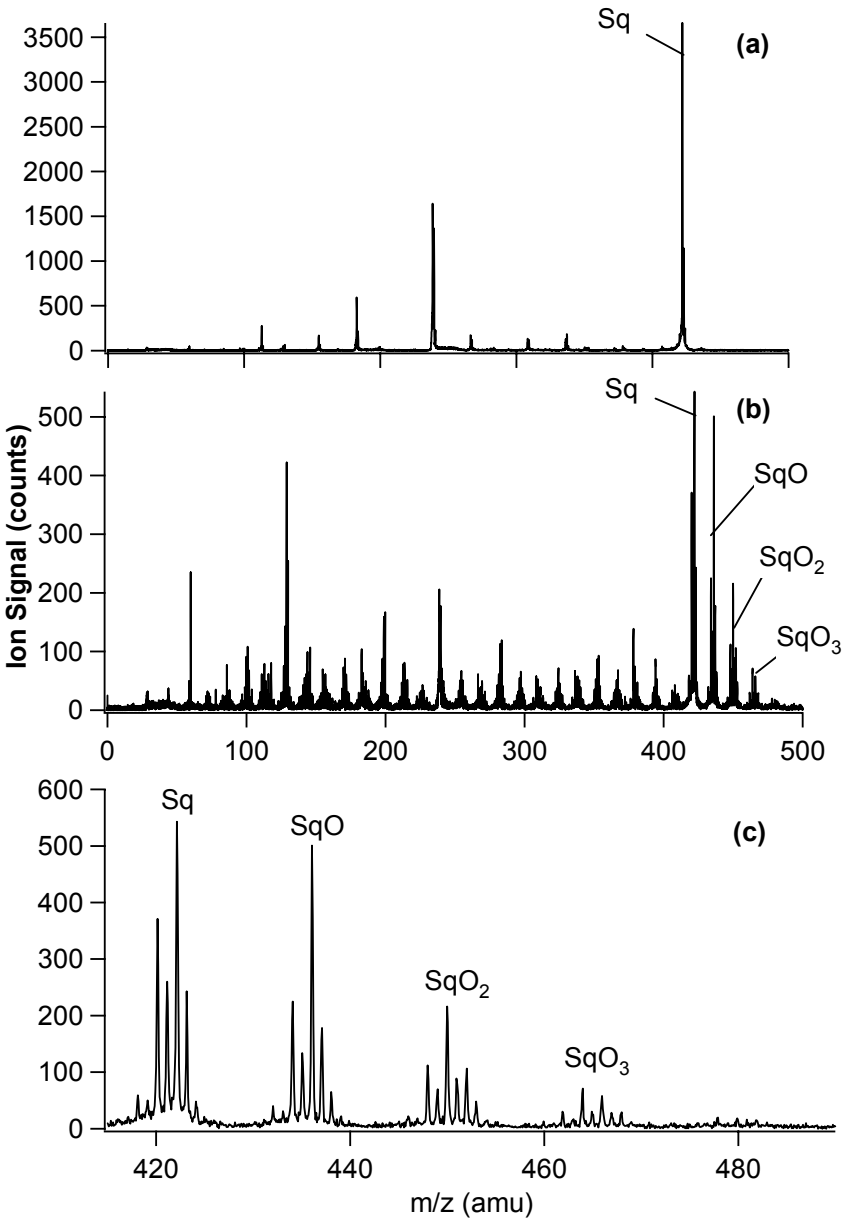
Sq
(a)
3500
3000
2500
2000
1500
1000
500
0
Sq
(b)
SqO
SqO_2
SqO_3
Ion Signal (counts)
500
400
300
200
100
0
0
100
200
300
400
500
Sq
SqO
(c)
SqO_2
SqO_3
600
500
400
300
200
100
0
420
440
460
480
m/z (amu)

Fig. 3

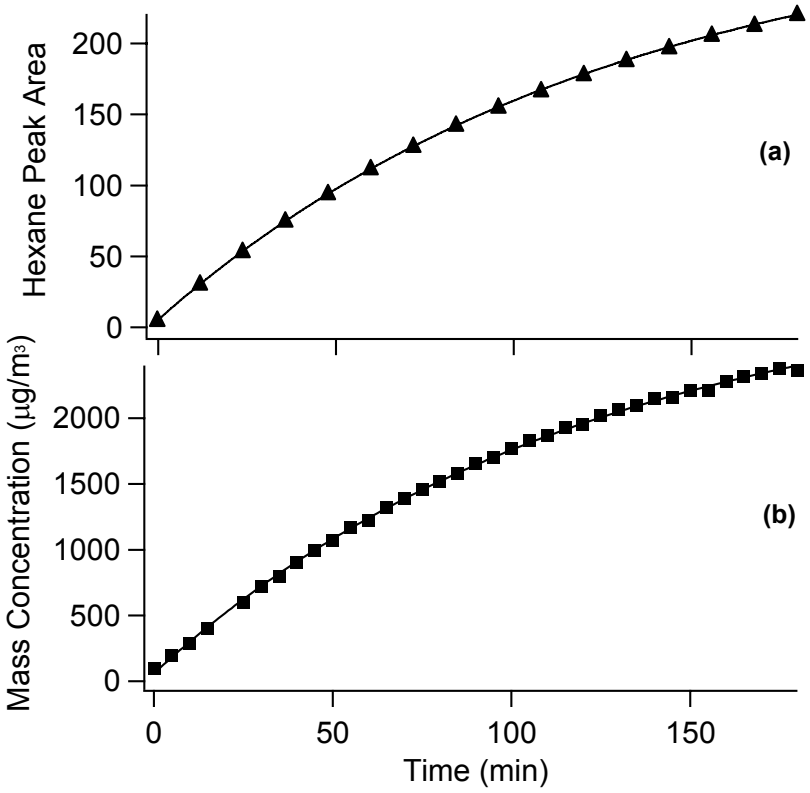
Hexane Peak Area
200
150
100
50
0
(a)
Mass Concentration (μg/m3)
2000
1500
1000
500
0
(b)
0
50
100
150
Time (min)

Fig. 4

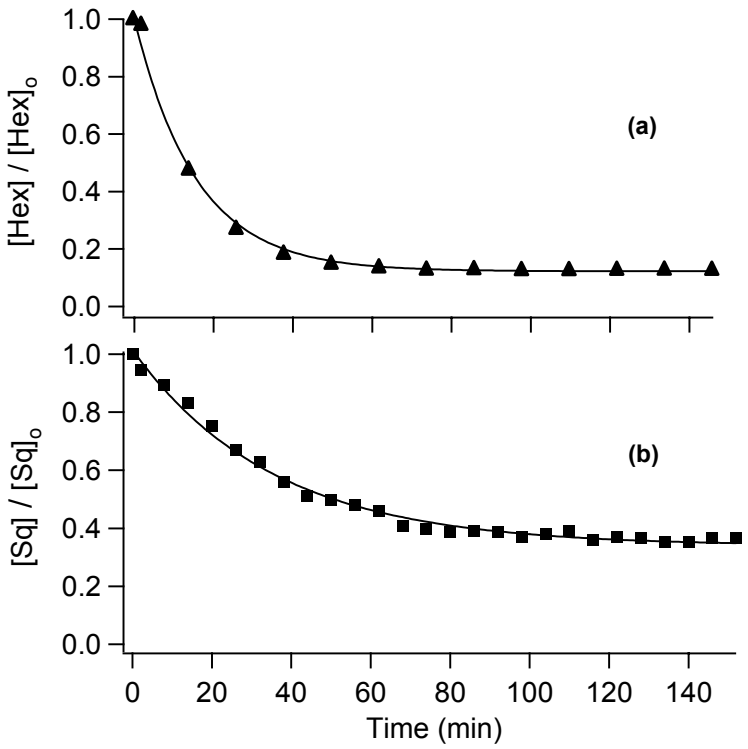
1.0
0.8
0.6
0.4
0.2
0.0
[Hex] / [Hex]o
(a)
1.0
0.8
0.6
0.4
0.2
0.0
[Sq] / [Sq]o
(b)
0
20
40
60
80
100
120
140
Time (min)

Fig. 5

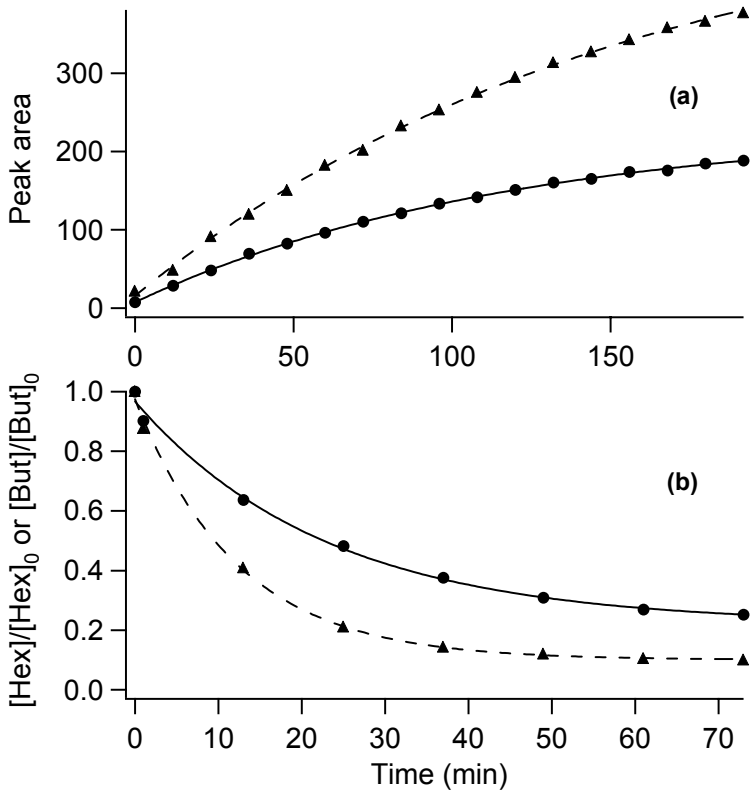
Peak area
300
200
100
0
0
50
100
150
(a)
[Hex]/[Hex]$_0$ or [But]/[But]$_0$
1.0
0.8
0.6
0.4
0.2
0.0
0
10
20
30
40
50
60
70
Time (min)
(b)

Fig. 6

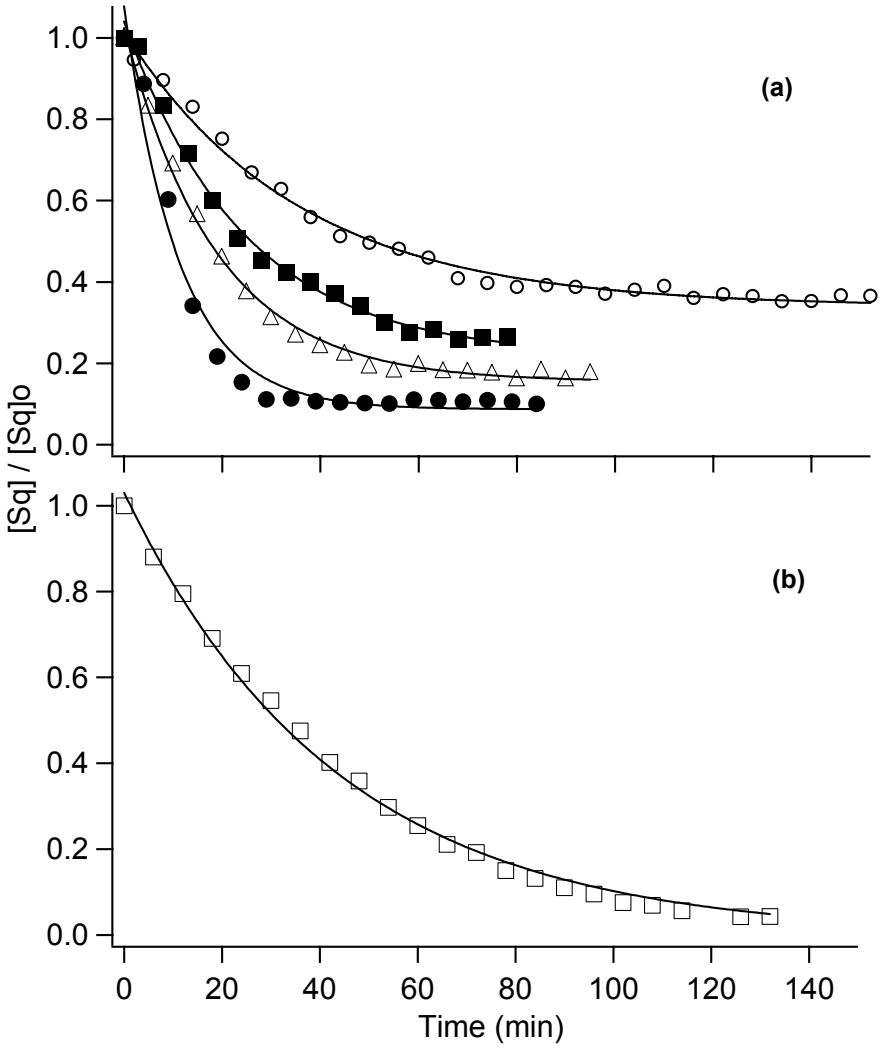
1.0
0.8
0.6
0.4
0.2
0.0
(a)
[Sq] / [Sq]o
1.0
0.8
0.6
0.4
0.2
0.0
(b)
0
20
40
60
80
100
120
140
Time (min)

Fig. 7

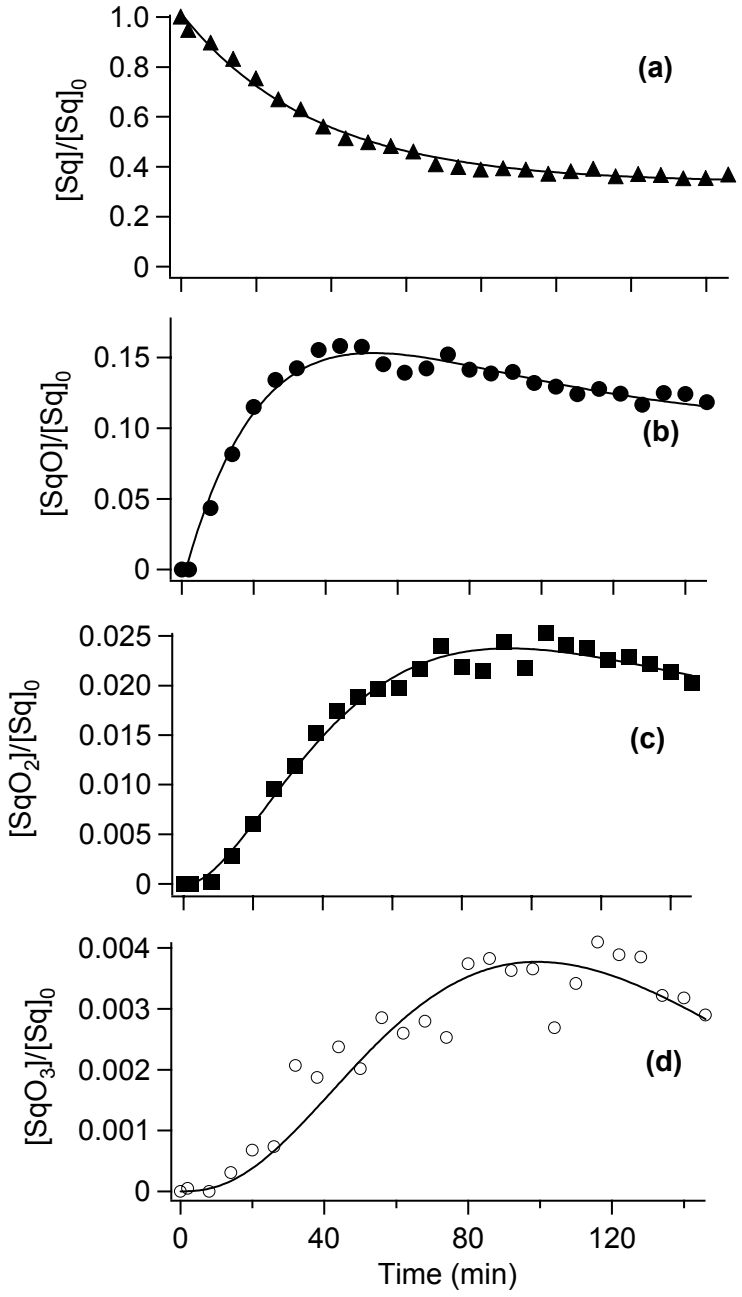
1.0
0.8
0.6
0.4
0.2
0
[Sq]/[Sq]0
(a)
0.15
0.10
0.05
0
[SqO]/[Sq]0
(b)
0.025
0.020
0.015
0.010
0.005
0
[SqO2]/[Sq]0
(c)
0.004
0.003
0.002
0.001
0
[SqO3]/[Sq]0
(d)
0
40
80
120
Time (min)

Fig. 8